

Quasi-Realistic Performance Analysis of Modern Atkinson Cycle

A. Onur Özdemir^{1*}, Latif K. Uysal¹, Regaip Menküç¹, Emre Arabacı²

0000-0002-6475-1976, 0000-0002-9182-5416, 0000-0002-2108-2418, 0000-0002-6219-7246

¹Automotive Engineering Department, Faculty of Technology, Gazi University, Ankara, 06500, Turkey

²Department of Automotive Engineering, Faculty of Technology, Pamukkale University, Denizli, 20160 Turkey

Abstract

In this study, a quasi-realistic thermodynamic analysis was performed to investigate the effects of design and operating parameters on the performance of a single-cylinder modern Atkinson cycle engine. Fortran was used for all calculations. It was assumed that the fuel-air mixture was used as the working fluid, and iso-octane was used as the fuel. The Wiebe function was used for the combustion process and it was assumed that the specific heat of the working fluid varies with temperature. In the calculations, heat transfer loss, combustion efficiency, mechanical friction, and pumping losses were taken into account. In the analysis, the closing of the intake valve, equivalence ratio, geometric compression ratio, and the initial conditions of the intake proses were used as independent variables. The effects of these variables on brake mean effective pressure, effective power, specific fuel consumption, and thermal efficiency were investigated. Increasing the inlet pressure, increasing the geometric compression ratio, and delaying the closing of the intake valve increased the mean effective pressure, thermal efficiency, engine output power, and torque. The increase in the inlet temperature adversely affected the engine performance and the specific fuel consumption increased. Engine performance parameters worsened when the equivalence ratio fell below 0.8 and rose above 0.9.

Keywords: Geometric compression ratio; Inlet temperature and pressure; Late intake valve closing; Modern Atkinson cycle.

Research Article

<https://doi.org/10.30939/ijastech..1184658>

Received 05.10.2022

Revised 31.10.2022

Accepted 10.11.2022

* Corresponding author

A. Onur Özdemir

onurozdemir@gazi.edu.tr

Address: Automotive Engineering Department, Faculty of Technology, Gazi University, Ankara, Turkey

Tel: +903122028653

1. Introduction

The basic energy sources we use are running out rapidly, and human beings are constantly researching to solve this problem. Various studies are ongoing worldwide to reduce dependence on fossil-based fuels and even destroy dependence on fossil fuels [1]. Greenhouse gases are seen as the main factor of global warming and abrupt climate changes that more clearly show their effects in the water-energy nexus. The exhaust emission caused by millions of fossil fuel vehicles used worldwide shows that it is one of the biggest triggers of the global climate change problem. In addition, vehicle emissions are seen as the cause of photochemical smog and haze [2]. Reducing dependence on fossil fuels used as the primary energy source in internal combustion engines will indirectly reduce emissions from vehicles. For this reason, vehicle manufacturers and researchers have worked to develop alternative energy sources and increase engine efficiency in recent years. Stricter standards are emerging in terms of fuel economy and emissions due to energy and environmental safety issues. To achieve these

limitations, the automotive industry is constantly introducing technological innovations. The production difficulty brought by emission standards forced the industry to leave diesel engines, especially in passenger cars. Approximately 96% of the passenger cars produced in 2017 were powered by a gasoline engine [3]. Although the emission and efficiency improvement efforts in internal combustion engines continue rapidly, due to the difficulty of this improvement process, the dissemination of electric and hybrid-electric vehicles is especially important [4-6]. Although problems such as battery life and the short range of electric vehicles are partially solved, an effective effort is still being made for these problems. In addition, modern Atkinson cycle engines are used in hybrid-electric vehicles offered by companies such as Toyota [7, 8] and Ford [9] today. In hybrid-electric vehicles, the internal combustion engine is generally operated under certain load and speed conditions to provide the best efficiency, thus ensuring both fuel economy and emissions [6, 8].

The Atkinson cycle was first created with a complex crank

mechanism developed by James Atkinson in 1882 [10]. Although this design was shown in the late 19th century, it has not been developed for a long time because it has a complex mechanism compared to conventional engine cycles [11]. Instead of using the complex crank mechanism in Atkinson's original design, the modern Atkinson cycle engine used in today's hybrid-electric vehicles is obtained by modifying the timing of the valves in the conventional engine. However, there are many studies for Atkinson cycle engines with a multi-link crank mechanism, similar to Atkinson's complex crank mechanisms [12-14]. Studies were also carried out on the Atkinson engine cycle, where the planetary gear mechanism is used instead of the Multi-Link crank mechanism [15]. One of the methods to achieve the Atkinson cycle is Variable Valve Timing (VVT). This VVT is generally applied to the intake valve. This method, obtained by changing the effective compression ratio in the delay or advanced state of the intake valve, is quite simple and practical compared to the multi-link crank mechanism. In this way, volumetric efficiency improves, but power density decreases dramatically [16-19]. Increasing the Geometric Compression Ratio (GCR) with VVT extends the expansion stroke. Thus, it was reported that some improvement in the power density decreased due to VVT [20-22]. This VVT+GCR method is most preferred in today's modern Atkinson cycle engines.

Many studies have been presented in which the effects of changing parameters such as valve timing, ignition advance, effective compression ratio, and geometric compression ratio were analyzed when the engine operates at various loads and speeds. Kentfield reported that when the rate of expansion was increased by 1.4 in a diesel engine cycle, the braking average effective pressure decreased, while there was an 8% improvement in brake-specific fuel consumption [23]. In diesel engines, the Late Intake Valve Closing (LIVC) method, which reduces the effective compression ratio compared to the expansion ratio, is frequently preferred. Using this LIVC method, Sakata achieved an Atkinson cycle motor with an effective compression ratio of 8.5 and an expansion ratio of 10.9. Sakata reported that the brake average effective pressure of 7 bar for a speed of 2500 rpm was an improvement of 18% in brake-specific fuel consumption [24]. Ust made a detailed analysis of the Atkinson cycle in the condition of maximum power density. Ust presented the conclusion that the Atkinson cycle is superior in terms of engine dimensions and thermal efficiency [25]. Yamada reported that thermal efficiency can be improved by reducing exhaust gas recirculation and friction in an Atkinson cycle engine with a high compression ratio [26]. Gahruei et al. created a detailed mathematical model to determine the effect of friction heat transfer on the Dual-Atkinson cycle performance [27]. A detailed study was carried out by Liu et al. on the fuel injection pressure, injection pressure, and Exhaust Gas Recirculation (EGR) ratio in an Atkinson cycle engine, and the combustion, emission, and performance parameters were investigated. Accordingly, it was observed that injection pressure had little effect on engine performance, but had a large effect on emissions. Injection timing was observed to have a significant impact on both performance and emissions [28]. In the study by Cinar et al., an Otto cycle engine was converted to an Atkinson cycle engine using the method of LIVC and increasing

the compression ratio. For this, first of all, thermodynamic analyzes were made, and a new camshaft was designed and produced for experimental work. In experimental studies, basic performance parameters were investigated depending on compression ratio and intake valve timing [29]. Liu et al. studied the effect of injection parameters of an Atkinson cycle gasoline engine on emission performance [30]. Some scholars proposed the Genetic Algorithm (GA) for the performance optimizations of heat engines. Li et al improved a non-dominated sorting GA model that provides fuel economy taking into account emissions targets [31]. Shi et al designed a multi-objective GA to determine the thermal efficiency corresponding to the maximum power of an irreversible Atkinson cycle when the specific heats were assumed constant [32].

In this study, a quasi-realistic thermodynamic analysis model was created for an Atkinson cycle single-cylinder spark-ignition engine. Considering the combustion efficiency, heat losses, and mechanical friction loss, the effects of intake valve closure, compression ratio, equivalence ratio, inlet pressure, and inlet temperature on engine performance were examined.

2. Theoretical Model

The theoretical (also called ideal or reversible) Atkinson cycle consists of isentropic compression (1-2), constant volume heat input (2-3), isentropic expansion (3-4), and constant pressure heat rejection (4-1) processes (Figure 1).

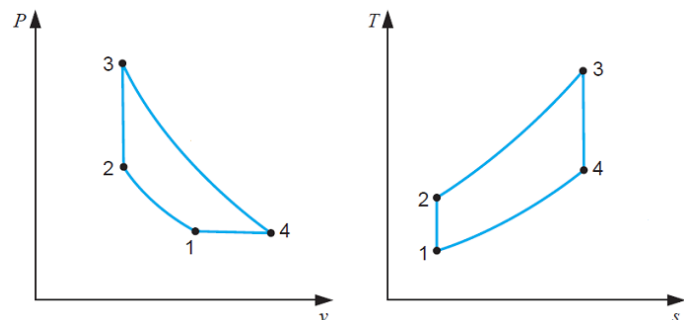


Fig. 1. P-v and T-s diagrams of irreversible Atkinson cycle

Theoretical cycles are not realistic because they are dimensionless models. Models that provide the characteristics of a real engine, and the use of realistic engine parameters are called quasi-realistic models. Also, it is assumed that the cycle working fluid is a mixture of air-fuel or air-fuel-residual gas instead of ideal air, and the specific heat of the working fluid varies depending on temperature. In this way, the theoretical model is upgraded to the quasi-realistic model, making it closer to the actual cycle. In the model, the LIVC method of the Atkinson cycle engine was applied.

Fortran program was used in the calculation model for the quasi-realistic Atkinson cycle engine. For the model, the cylinder diameter (D) was assumed to be 0.075 m, stroke length (Ls) 0.0847 m, and connecting rod length (Lc) 0.148 m. The lower thermal value (Hu) of the fuel was 44425 kJ/kg, and the coolant temperature was accepted as constant 360 K. The flow diagram of the analysis model is presented in Figure 2.

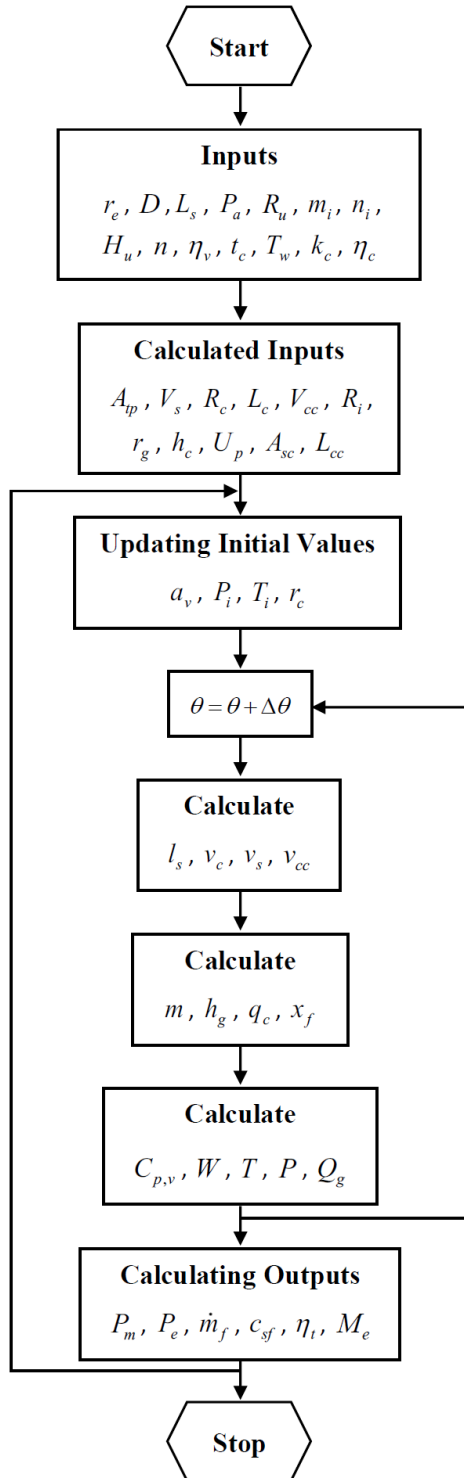


Fig. 2. Analysis flow chart

In-cylinder pressure and temperature values were determined in one-degree crank angle intervals. All engine characteristics were obtained for a constant engine speed of 3000 rpm. In cycle analysis, heat losses, mechanical friction losses, pumping losses, and combustion efficiency were included in the calculations. Exhaust gases (residual gases) from the previous cycle were neglected, but the

inlet pressure and temperature were changed. In addition, the effects on engine performance were investigated by changing the equivalence ratio, intake valve closure, and geometric compression ratio. The equations used in model calculations are presented below.

To find the instantaneous stroke volume, the linear displacement of the piston in the cylinder was calculated [33]:

$$L_s = R_c + L_c - \left(R_c \cdot \cos \theta + \sqrt{L_c^2 - R_c^2 \cdot \sin^2 \theta} \right) \quad (1)$$

To determine the mass of the mixture, the mass of each gas was calculated, based on the mole percent ratios:

$$m_g = \frac{P \cdot V}{R_i \cdot T} \cdot \eta_v \cdot x(\%) \quad (2)$$

Fuel-air mixture was used as working fluid in the cycle, and the fuel was considered to be iso-octane (C8H18). Ignition advance was assumed to be 20o crank angle before TDC and combustion duration was 40o crank angle. In addition, it was assumed that the heat distribution occurred according to the Wiebe function:

$$x_f = 1 - \exp \left[-w \left(\frac{\theta - \theta_0}{d\theta} \right)^{z+1} \right] \quad (3)$$

where w and z are constant coefficients [34]. Combustion efficiency is expressed as follows [35]:

$$\eta_c = -1.4473 + 4.1858 \cdot \phi - 1.8687 \cdot \phi^2 \quad (4)$$

where, ϕ is the equivalence ratio, the stoichiometric ratio divided by the actual air-fuel ratio. The variation of specific heats with temperature for each gas and fuel was calculated with the following equations:

$$C_{p,g} = R_i \left[a_{x1} + a_{x2}T + a_{x3}T^2 + a_{x4}T^3 + a_{x5}T^4 \right] \quad (5)$$

$$C_{p,f} = \frac{A_{y1} + A_{y2} \frac{T}{1000} + A_{y3} \left(\frac{T}{1000} \right)^2 + A_{y4} \left(\frac{T}{1000} \right)^3 + A_{y5} \left(\frac{1000}{T} \right)^2}{m} \quad (6)$$

a_x and A_y values in these equations were taken from the Janaf Tables [35]. Eq. (7) was used for the convective heat transfer coefficient in the cylinder [36]:

$$h_g = 3.26 \cdot D^{-0.2} \cdot P^{0.8} \cdot T^{-0.55} \cdot (2.28 \cdot U_p)^{0.8} \quad (7)$$

The mean cycle pressure was calculated as follows:

$$P_m = \frac{W}{V_s} \quad (8)$$

The power lost due to mechanical friction was calculated as follows [37]:

$$N_f = 0.0129 \left(\frac{2 \cdot n}{60} \cdot L_s \right)^2 \tag{9}$$

The following equations were used for power and torque:

$$P_e = \frac{P_m \cdot V_s \cdot n}{120} \tag{10}$$

$$M_e = \frac{60 \cdot P_e}{2 \cdot \pi \cdot n} \cdot 1000 \tag{11}$$

Specific fuel consumption was calculated as:

$$C_{sf} = \frac{\dot{m}_f}{P_e} \tag{12}$$

The thermal efficiency was defined as:

$$\eta_t = \frac{120 \cdot P_e}{n \cdot f_c \cdot H_u} \tag{13}$$

The specifications used in the analytical model are given in Table 1.

Table 1. Details of analysis

Item	Value
Cylinder diameter (m)	0.075
Stroke length (m)	0.0847
Connecting rod length (m)	0.148
Working fluid	<i>iso-octane</i>
Lower thermal value of the fuel (kJ/kg)	44425
Coolant temperature (K)	360
Ignition advance (crank angle)	20° before TDC
Combustion duration (crank angle)	40°
Heat losses	<i>calculated</i>
Mechanical friction losses	<i>calculated</i>
Pumping losses	<i>calculated</i>
Combustion efficiency	<i>calculated</i>
Variation of specific heats with temperature	<i>calculated</i>
Residual gases	<i>neglected</i>
Inlet pressure (bar)	<i>changed from 0.9 to 1.40</i>
Inlet temperature (K)	<i>changed from 298 to 548</i>
Intake valve closing (crank angle)	<i>changed from 180 to 270</i>
Geometric compression ratio	<i>changed from 7 to 19</i>
Equivalence ratio	<i>changed from 0.7 to 1.4</i>

3. Results and Discussion

The compression ratio, intake valve closing, cylinder wall temperature, and atmospheric pressure values accepted as a reference in this study are 13, 360 K, 253o crank angle, and 101.325 Pa, respectively. As a result of calculations with a 1-degree crank angle step, engine performance parameters were calculated. Below, various graphs were obtained to examine the effects of inlet pressure, inlet temperature, equivalence ratio, geometric compression ratio, and intake valve closing on engine power, engine torque, thermal efficiency, and specific fuel consumption.

The change of the mean effective pressure depending on the cycle initial conditions (pressure and temperature values of point 1 in Figure 1) is shown in Figure 3. When the initial pressure was examined between 0.9-1.4 bar and the initial temperature was constant at 360 K, it was seen that the mean effective pressure increased with increasing initial pressure. Likewise, when the initial pressure was at 1.0 bar and the initial pressure was constant at 1.0 bar, it was observed that the mean effective pressure decreased with increasing temperature. The average effective pressure for 1.0 bar and 360 K initial conditions was determined as 713.2 kPa.

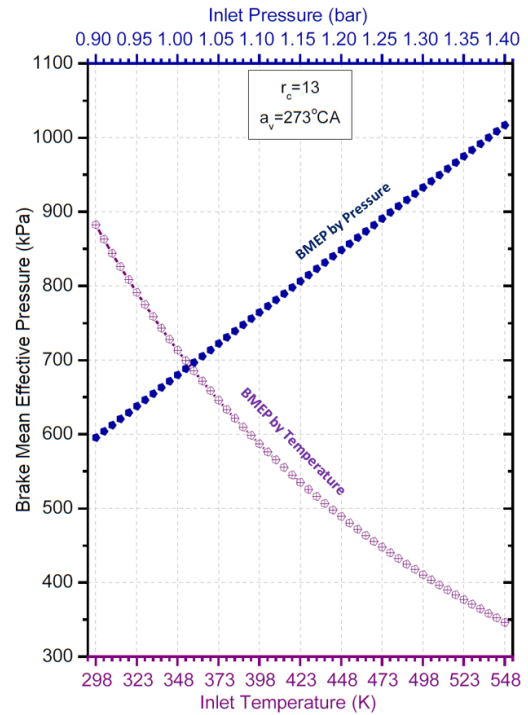


Fig. 3. Brake mean effective pressure as functions of initial pressure and initial temperature

The effect of the cycle initial temperature and initial pressure on engine performance are presented in Figure 4 and Figure 5, respectively. The initial temperature varies depending on the operating conditions and the amount of residual gas. Since the heat losses increase with the increase of the initial temperature, the thermal efficiency decreases, and the specific fuel consumption increases. In addition, the mass of the cycle working fluid (air-fuel mixture) decreases as the initial temperature increases. For this reason, the

combustion energy also decreases, thus the engine power and engine torque decrease dramatically. For 298 K initial temperature, engine power, engine torque, thermal efficiency, and specific fuel consumption are determined as 8.2 kW, 26.2 Nm, 35.5%, and 227.9 g/kWh, respectively, when the initial temperature is increased to 548 K, the same data are determined as 3.2 kW, 10.3 Nm, 25.6% and 315.8 g/kWh, respectively. That is when the initial

temperature was increased from 298 K to 548 K, engine power and engine torque decreased by approximately 61%, and specific fuel consumption increased by approximately 31%. Increasing the inlet temperature causes a decrease in the density of the mixture and a decrease in the mass of the mixture taken into the cylinder per unit volume. Thus, as the volumetric efficiency decreases, the engine torque declines, and the specific fuel consumption increases.

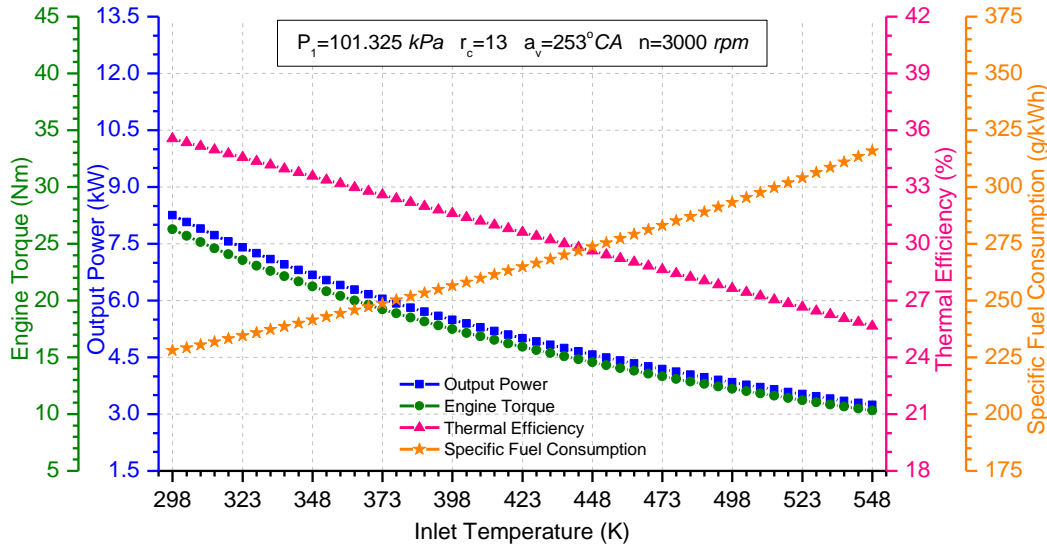


Fig. 4. The engine performance versus inlet temperature

While the atmospheric pressure at sea level is 1.0 bar, it decreases to 0.9 bar at 1000 m altitude above sea level [38]. This low pressure creates resistance when the working fluid is taken into the cylinder. Engine power, engine torque, thermal efficiency, and specific fuel consumption for 0.9 bar initial pressure are determined as 5.5 kW, 17.7 Nm, 32.1%, and 251.6 g/kWh, respectively. Over-charged (supercharge, turbocharge, etc.) systems increase initial pressure up to 1.4 bar in order to compensate for variable atmospheric conditions and improve volumetric

efficiency. Increasing the amount of air without changing the equivalence ratio also increases the fuel energy in the cycle. Thus, with the increase of combustion energy, engine power and engine torque increase with increasing initial pressure. Similarly, specific fuel consumption decreases as the initial pressure increases. Engine power, engine torque, thermal efficiency, and specific fuel consumption for 1.4 bar inlet pressure are determined as 9.5 kW, 30.2 Nm, 35.3%, and 229.2 g/kWh, respectively.

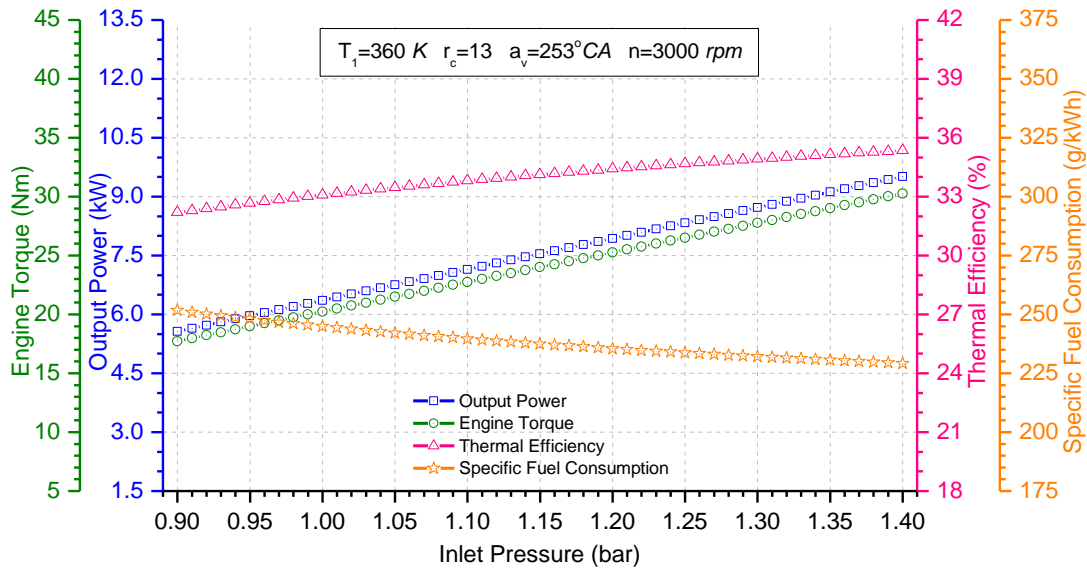


Fig. 5. Performance curves versus inlet pressure

The effects of compression ratio change on engine performance are shown in Figure 6. It was assumed that the amount of fuel used in one cycle remains constant (0.0173 g). The effective compression ratio is changed by closing the inlet valve later than normal (253° crank angle). It was observed that engine performance improved with increasing compression ratio. When the compression ratio is increased, the stroke volume also increases. Cooling heat transfer is also increased due to the increased surface area of the cylinder. With the increase in the stroke volume, the expansion process in which positive work was achieved increased, and the thermal efficiency increased. However, with the

increased surface area of the piston, an increase in mechanical friction also occurred. In a conventional Otto cycle engine, theoretically, the intake valve is assumed to close when the piston is at the bottom dead center, in which case the geometric and actual compression ratio is limited to 9.5. In an Atkinson cycle engine designed with a geometric compression ratio of 13, the intake valve is closed at a 253° crank angle, and the effective compression ratio is reduced to 9.5, as in the Otto cycle engine. For these conditions, engine power, engine torque, thermal efficiency, and specific fuel consumption are determined as 6.4 kW, 20.4 Nm, 33.4%, and 242.4 g/kWh, respectively.

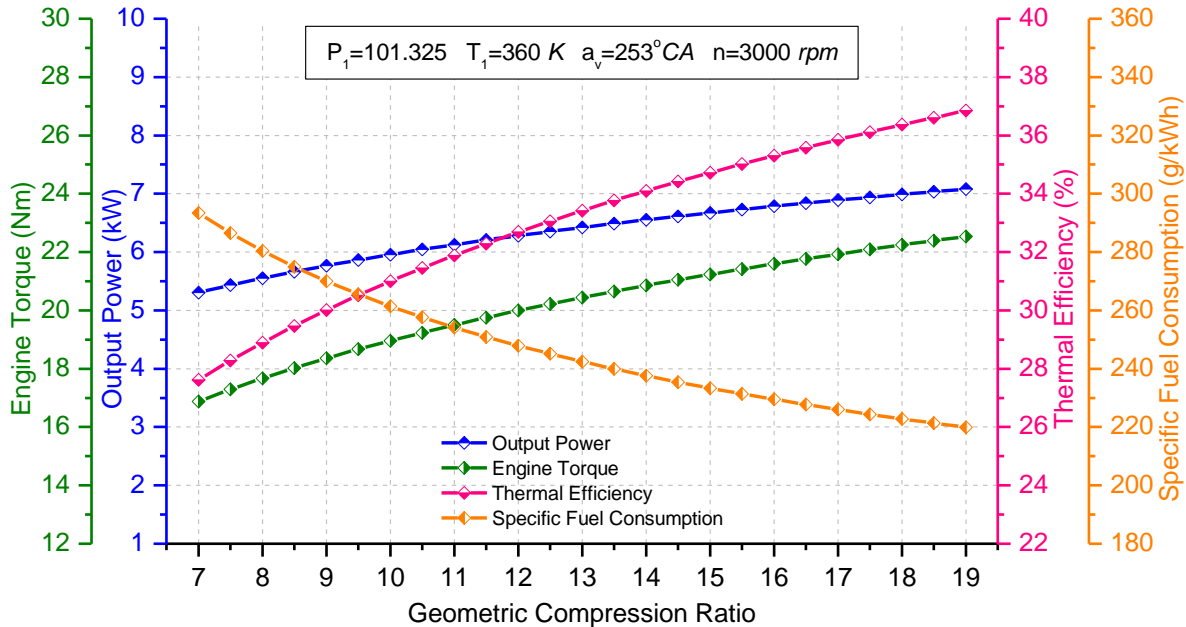


Fig. 6. The variation of the engine performance with a geometric compression ratio

The effects of late intake valve closing on engine performance are presented in Figure 7. When the geometric compression ratio is constant, the intake valve closure was changed between 180-273° crank angle so that the effective compression ratio can be achieved between 13-7. Accordingly, the mass of fuel entering the cylinder in one cycle ranged from 0.0130-0.0242. Increasing the intake valve delay causes some of the working fluid that enters the cylinder to return to the intake manifold, thereby reducing the engine torque. The effective compression ratio decreases as the intake valve delay increases. For this reason, the compression pressure and thus the mean effective pressure were reduced. For this reason, the maximum engine power and engine torque were realized at 180 kW and 26.8 Nm, respectively. Increasing

the intake valve delay causes the pumping loss to decrease as it reduces the effective compression ratio. As the expansion process is longer than the compression process, an improvement in thermal efficiency and therefore specific fuel consumption was achieved. When the intake valve is closed at a 273° crank angle, engine power, engine torque, thermal efficiency, and specific fuel consumption are determined as 5.1 kW, 16.4 Nm, 35.0%, and 31.4 g/kWh, respectively. Murtaza also presented similar results [39]. When the late intake valve closing was delayed from 180 to 273 crank angle, engine torque and engine power decreased by 39%, whereas thermal efficiency and specific fuel consumption improved by about 13%.

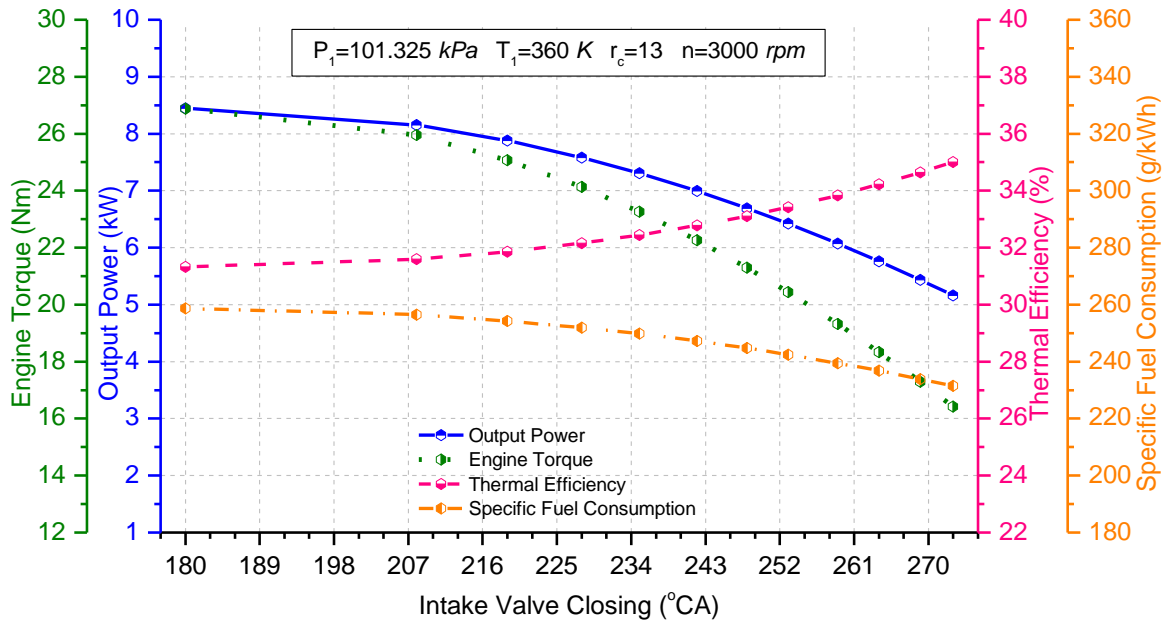


Fig. 7. Influences of the late intake valve closing on the engine performance

The effect of equivalence ratio and suction valve closure on engine power and engine torque is as in Figure 8. When the equivalence ratio is less than one, it refers to the lean mixture, and when it is more than one, it means the rich mixture. The most engine power and engine torque were obtained when the equivalence ratio was 0.9. Engine power and engine torque are

reduced as the intake valve closing is delayed. If the equivalence ratio is 0.9, engine power and engine torque are 5.2 kW and 16.7 Nm, respectively, when the intake valve closing is 273o crank angle, and engine power and engine torque increase approximately 65% when the intake valve closing is 180o crank angle, respectively.

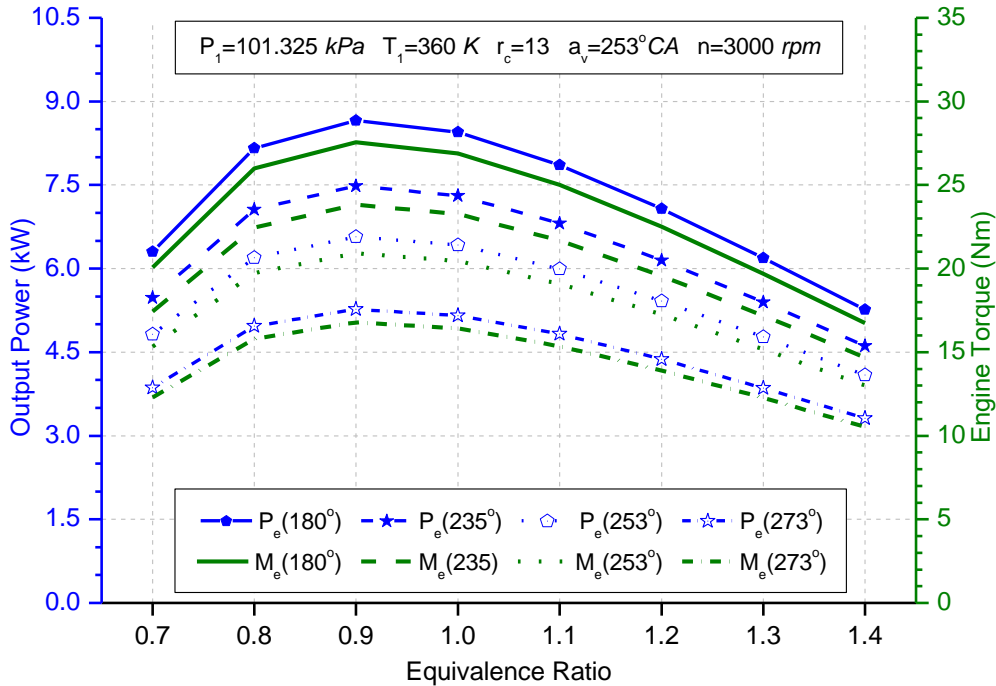


Fig. 8. Effect of equivalence ratio on the power and torque with variable valve timing

The effect of intake valve closing and equivalence ratio on thermal efficiency and specific fuel consumption is presented in Figure 9. The equivalence ratio was changed between 0.7-1.4. While the equivalence ratio was 0.8, maximum thermal efficiency was obtained. Heat efficiency and specific fuel consumption improve as the intake valve closing is delayed. In case the equivalence ratio is 0.8, the thermal efficiency is 42.1% when

the intake valve closing is 273 and the specific fuel consumption is 192.3 g/kWh. Similar to this result, Gonca stated that in his paper, the performance parameters increased to a certain value and then started to decrease with an increasing equivalence rate. He reported that the low and high equivalent rates of thermal efficiency and the decrease in specific fuel consumption were due to low fuel energy input [40].

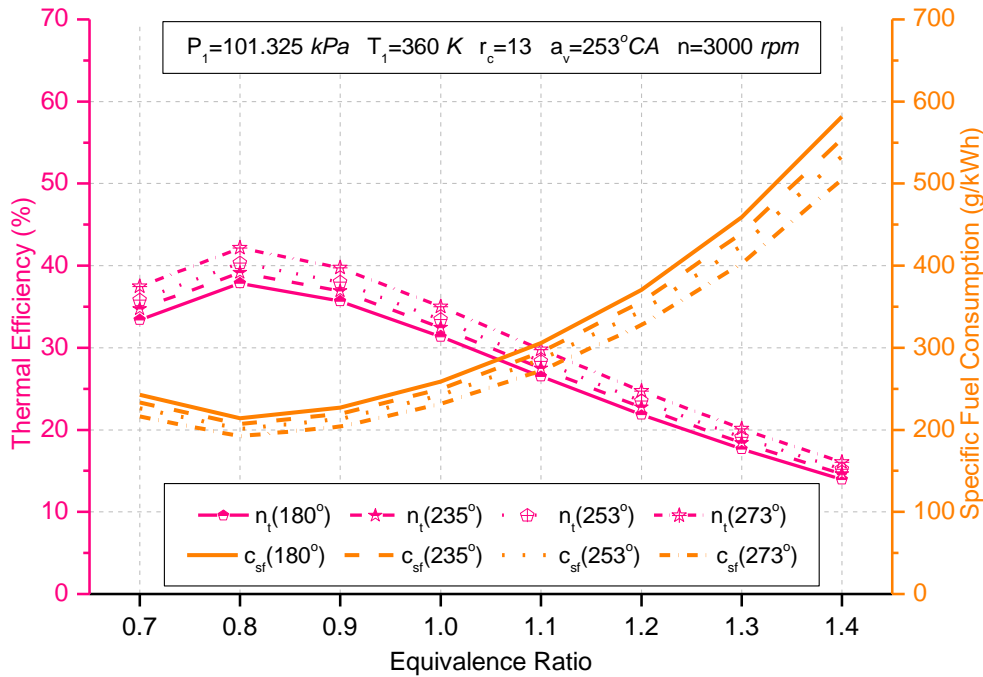


Fig. 9. Effect of equivalence ratio on the efficiency and fuel consumption with variable valve timing

4. Conclusion

In this study, a thermodynamic analysis model was developed for an Atkinson cycle engine, depending on the compression ratio, equivalence rate, intake valve closing time, inlet temperature and inlet pressure change, the engine power, engine torque, mean effective pressure, specific fuel consumption and thermal efficiency of this engine. Effects were investigated parametrically. The results are presented below:

- The mean effective pressure increased with the increase of the inlet pressure, and the increase of the inlet temperature caused a decrease in mean effective pressure.
- Increasing inlet temperature negatively affected engine performance, and as the temperature increased, output power, torque, and thermal efficiency reduced and specific fuel consumption increased.
- Increasing inlet pressure led to an improvement in performance characteristics; as pressure increased, output power, torque, and thermal efficiency increased, and specific fuel consumption decreased.

- As the geometric compression ratio increased, there was a significant improvement in engine output power, torque, thermal efficiency, and specific fuel consumption.
- As the closing of the intake valve was delayed, while the engine output power and torque decreased, the thermal efficiency increased, and the specific fuel consumption decreased.
- It was found that performance parameters improved up to a certain equivalence ratio, and then increased equivalence ratio negatively affected combustion efficiency and worsened engine performance.

Nomenclature

- A_{sc} : Cylinder surface area (m²)
- A_{tp} : Piston top surface area (m²)
- a_v : Intake valve closing (°CA)
- f_c : Mass of fuel per cycle (kg)
- CA : Crank angle
- C_{pf} : Specific heat of the fuel (kJ/kgK)
- C_{pg} : Specific heat of the gas (kJ/kgK)

$C_{p,v}$: Specific heat of the mixture (kJ/kgK)
c_{sf}	: Specific fuel consumption (kJ/kgK)
D	: Cylinder bore (m)
$d\theta$: Combustion duration (°CA)
h_c	: Convective heat transfer coefficient of coolant (W/m ² K)
h_g	: Convective heat transfer coefficient of mixture (W/m ² K)
H_u	: Lower heating value of the fuel (kJ/kg)
k_c	: Thermal conductivity of cylinder (W/mK)
L_c	: Connecting rod length (m)
L_{cc}	: Combustion chamber length (m)
l_s	: Changing stroke length (m)
L_s	: Stroke length (m)
M_e	: Engine torque (Nm)
m	: Mixture mass taken into the cylinder (kg)
m_g	: Gas mass (kg)
m_i	: Molecular mass (kg/kmol)
\dot{m}_f	: Mass flow rate of fuel (kg/h)
n	: Engine speed (min ⁻¹)
N_f	: Mechanical friction power (kW)
n_i	: Mole numbers (kmol)
P	: Pressure (Pa)
P_a	: Atmospheric pressure (Pa)
P_e	: Output power (kW)
P_i	: Inlet pressure (Pa)
P_m	: Mean cycle pressure (Pa)
q_c	: Lost heat (kJ)
Q_g	: Entering heat (kJ)
R_c	: Crank radius (m)
r_c	: Geometric compression ratio
r_e	: Expansion ratio
r_g	: Gas percentages
R_i	: Gas constants (kJ/kgK)
R_u	: Universal gas constant (kJ/kmolK)
T	: Temperature (K)
t_c	: Cylinder wall thickness (m)
T_i	: Inlet temperature (K)
T_w	: Average temperature (K)
U_p	: Mean piston speed (m/s)
V	: Volume (m ³)
v_c	: Changing cylinder volume (m ³)
v_{cc}	: Changing combustion chamber volume (m ³)
V_{cc}	: Combustion chamber volume (m ³)

v_s	: Changing stroke volume (m ³)
V_s	: Stroke volume (m ³)
W	: Work (kJ)
x_f	: Mass fraction burned
θ	: Crankshaft angle (°)
θ_0	: Start of combustion (°CA)
ϕ	: Equivalence ratio
η_c	: Combustion efficiency
η_t	: Thermal efficiency
η_v	: Volumetric efficiency

Conflict of Interest Statement

The authors declare that there is no conflict of interest in the study.

CRedit Author Statement

A. Onur Özdemir: Conceptualization, Methodology, Software, Writing-original draft.

Latif K. Uysal: Writing - original draft, Visualization.

Regaip Menküç: Data curation.

Emre Arabacı: Supervision, Writing-review&editing.

References

- [1] Fu J, Liu J, Feng R, Yang Y, Wang L, Wang Y. Energy and exergy analysis on gasoline engine based on mapping characteristics experiment. *Applied Energy*, 2013; 102: 622-630.
- [2] Zhao J. Research and application of over-expansion cycle (Atkinson and Miller) engines. *Applied Energy*, 2017; 185: 300-319.
- [3] Huntchings I, Shipway P. *Tribology: friction and wear of engineering materials*. Butterworth-Heinemann, 2017.
- [4] Demir A, Gümüş M, Sayın C, Boztoprak Y, Yılmaz M. Geçmişten günümüze otomobil teknolojileri. *Mimar ve Mühendis Dergisi*, 2012; 64: 60-63.
- [5] Leach F, Kalghatgi G, Stone R, Miles P. The scope for improving the efficiency and environmental impact of internal combustion engines. *Transportation Engineering*, 2020; 1: 100005.
- [6] Gheorghiu V. CO₂ - emission reduction by means of enhanced thermal conversion efficiency of ice cycles. *SAE Technical Paper*, 2009-24-0081.
- [7] Muta K, Yamazaki M, Tokieda J. Development of new-generation hybrid system Toyota Hybrid System (THS) II - drastic improvement of power performance and fuel economy. *SAE Technical Paper*, 2004-01-0064.
- [8] Wang Y, Biswas A, Rodriguez R, Keshavarz-Motamed Z, Emadi A. Hybrid electric vehicle specific engines: State-of-the-art review. *Energy Reports*, 2022; 8: 832-851.
- [9] Karden E, Ploumen S, Fricke B, Miller T, Snyder K. Energy storage devices for future hybrid electric vehicles. *Journal of Power Sources*, 2006; 16(1): 2-11.
- [10] Atkinson J. Atkinson engine. US Patent 367496, 1887.
- [11] Pertl P, Trattner A, Abis A, Schmidt S, Kirchberger R, Sato T.

- Expansion to higher efficiency - investigations of the Atkinson cycle in small combustion engines. SAE Technical Paper, [2012-32-0059](#).
- [12] Kono S, Koga H, Watanabe S. Research on extended expansion general-purpose engine-efficiency enhancement by natural gas operation. SAE Technical Paper, 2010-32-0007.
- [13] Yamada Y. Engine of compression-ratio variable stroke. US Patent 6820577, 2004.
- [14] Boretta A, Scalzo J. Exploring the advantages of Atkinson effects in variable compression ratio turbo GDI engines. SAE Technical Paper, 2011-01-0367.
- [15] Pertl P, Trattner A, Abis A, Schmidt S, Kirchberger R, Sato T. Expansion to higher efficiency - investigations of the Atkinson cycle in small combustion engines. SAE Technical Paper, 2012-32-0059.
- [16] Wang Y, Lin L, Zeng S, Huang J. Application of the Miller cycle to reduce NOx emissions from the petrol engines. *Applied Energy*, 2008; 85: 463-74.
- [17] Wang Y, Lin L, Anthony P. An analytic study of applying Miller cycle to reduce NOx emission from petrol engine. *Applied Thermal Engineering*, 2007; 27: 1779-89.
- [18] Gonca G, Sahin B, Parlak A, Ust Y, Ayhan V, Cesur I, Boru B. Theoretical and experimental investigation of the Miller cycle diesel engine in terms of performance and emission parameters. *Applied Energy*, 2015; 138: 11-20.
- [19] Sher E, Bar-Kohany T. Optimization of variable valve timing for maximizing performance of an unthrottled SI engine - a theoretical study. *Energy*, 2002; 27: 757-75.
- [20] Shiga S, Hirooka Y, Yagi S. Effects of over-expansion cycle in a spark-ignition engine using late-closing of intake valve and its thermodynamic consideration of the mechanism. *International Journal of Automotive Technology*, 2001; 2(1): 1-7.
- [21] Okamoto K, Zhang F, Shimogata S, Shoji F. Development of a late intake-valve closing (LIVC) Miller cycle for stationary natural gas engines-effects of EGR utilization. SAE Technical Paper, 1997; 972948.
- [22] Fukuzawa Y, Shimoda H, Kakuhma Y. Development of high efficiency Miller cycle gas engine. *Stroke*, 2001; 38(3): 146-50.
- [23] Kentfield JAC. Alternative mechanical arrangements for diesel and spark-ignition engines employing extended expansion strokes. SAE Technical Paper, 1992; 929060.
- [24] Sakata Y, Yamana K, Nishida K, Shimizu T, Shiga S, Araki M, Nakamura H, Obokata T. A study on optimization of an over-expansion cycle gasoline engine with late-closing of intake valves. 8th International Conference on Engines for Automobiles, Italy, 2007.
- [25] Yasin U. A comparative performance analysis and optimization of the irreversible Atkinson cycle under maximum power density and maximum power conditions. *International Journal of Thermophysics*, 2009; 30: 1001-1013.
- [26] Yamada T, Adachi S, Nakata K, Kurauchi T, Takagi I. Economy with superior thermal efficient combustion. SAE Technical Paper, 2014-01-1192.
- [27] Gahruei MH, Jeshvaghani HS, Vahidi S, Chen L. Mathematical modeling and comparison of air standard Dual and Dual-Atkinson cycles with friction, heat transfer and variable specific-heats of the working fluid. *Applied Mathematical Modelling*, 2013; 37(12-13): 7319-7329.
- [28] Liu Q, Guo T, Fu J, Dai H, Liu J. Experimental study on the effects of injection parameters and exhaust gas recirculation on combustion, emission and performance of Atkinson cycle gasoline direct-injection engine. *Energy*, 2022; 238: 121784.
- [29] Cinar C, Ozdemir AO, Gulcan HE, Topgül T. Theoretical and experimental investigation of the performance of an Atkinson cycle engine. *Arabian Journal for Science and Engineering*, 2021; 46(8): 7841-7850.
- [30] Liu Q, Guo T, Fu J, Dai H, Liu J. Experimental study on the effects of injection parameters and exhaust gas recirculation on combustion, emission and performance of Atkinson cycle gasoline direct-injection engine. *Energy*, 2022; 238: 121784.
- [31] Li Y, Wang S, Duan X, Liu S, Liu J, Hu S. Multi-objective energy management for Atkinson cycle engine and series hybrid electric vehicle based on evolutionary NSGA-II algorithm using digital twins. *Energy Conversion and Management*, 2021; 230: 113788.
- [32] Shi SS, Ge YL, Chen LG, Feng HJ. Four objective optimization of irreversible Atkinson cycle based on NSGA-II. *Entropy*, 2020; 22: 1150.
- [33] Abu-Nada E, Al-Hinti I, Al-Sarkhi A, Akash B. Thermodynamic modeling of spark ignition engine, effect of temperature dependent specific heats. *International Communications in Heat and Mass Transfer*, 2006; 33: 1264-1272.
- [34] Heywood JB. *Internal combustion engine fundamentals*. McGraw Hill Education, 2018.
- [35] Gonca G. Performance analysis of an Atkinson cycle engine under effective power and effective power density conditions. *Acta Physica Polonica A*, 2017; 132 (4): 1306-1313.
- [36] Shoukry E, Taylor S, Clark N, Famouri P. Numerical simulation for parametric study of a two-stroke direct injection linear engine. SAE Technical Paper, 2002-01-1739.
- [37] Lin JC, Hou SS. Effects of heat loss as percentage of fuel's energy, friction and variable specific heats of working fluid on performance of air standard Otto cycle. *Energy Conversion and Management*, 2008; 49: 1218-1227.
- [38] George S, Sreelal M, Saran S, Joseph S, Varghese AK. High altitude air flow regulation for automobiles. *International Conference on Recent Trends in Engineering Science and Management*, New Delhi, India, 2015.
- [39] Murtaza G, Bhatti AI, Ahmed Q. Control-oriented model of Atkinson cycle engine with variable intake valve actuation, *Journal of Dynamic Systems, Measurement, and Control*, 2016; 138: 06100/1-9.
- [40] Gonca G. Thermodynamic analysis and performance maps for the irreversible Dual-Atkinson cycle engine (DACE) with considerations of temperature-dependent specific heats, heat transfer and friction losses. *Energy Conversion and Management*, 2016; 111: 205-216.